

# Controlling Localized Plasmons via an Atomistic Approach: Attainment of Site-Selective Activation inside a Single Molecule

*Sayantan Mahapatra, Jeremy F. Schultz, Linfei Li\*, Xu Zhang, and Nan Jiang\**

## Abstract

Chemical reactions such as bond dissociation and formation assisted by localized surface plasmons (LSPs) of noble metal nanostructures hold promise in solar-to-chemical energy conversion. However, the precise control of localized plasmons to activate a specific moiety of a molecule, in the presence of multiple chemically equivalent parts within a single molecule, is scarce due to the relatively large lateral distribution of the plasmonic field. Herein, we report the plasmon-assisted dissociation of a specific molecular site (C—Si bond) within a poly-functional molecule adsorbed on a Cu(100) surface in the scanning tunneling microscope (STM) junction. The molecular site to be activated can be selected by carefully positioning the tip and bringing the tip extremely close to the molecule (atomistic approach), thereby achieving plasmonic nano-confinement at the tip apex. Furthermore, multiple reactive sites are activated one by one from the single molecular structure, and different sets of products are created and visualized by constant current topography and density functional theory (DFT) modeling. The illustration of site-selective activation probed by localized surface plasmons implies the realization of molecular-scale resolution for bond-selected plasmon-induced chemistry.

Localized surface plasmon (LSP) resonance, which is the collective oscillation of free electrons of noble metal nanostructures (such as Ag, Au, and Cu) coupled with the electric field of the incident light, has attracted paramount interest in recent years as an efficient driving force for energy conversion-related problems.<sup>1-7</sup> Recently, researchers have realized that chemical reactions can be effectively induced by localized plasmons via either the generation of hot charge carriers (such as electrons and holes) or the local heating effect.<sup>8-10</sup> Moreover, plasmon-mediated chemical reactions provide a promising approach over thermally induced processes as they can utilize light energy to drive a thermodynamically unfavorable reaction under mild conditions, therefore significantly reducing the energy requirements for chemical transformation.<sup>11-13</sup> For example, a strong nonpolarizable H—H bond can be dissociated on a gold nanoparticle through the injection of hot electrons into the  $\sigma^*$  orbital.<sup>14</sup>

Although chemical reactions assisted by LSPs have been extensively demonstrated in the past decade, the control of a localized plasmonic field towards the formation of desired products remains extremely difficult and thus challenging to attain. In order to address this, nanoscale investigations are required, which leads to the integration of the scanning tunneling microscope (STM) with optical excitation by light<sup>15-16</sup> and luminescence from the STM tip-sample junction.<sup>17-20</sup> Recently, combining light with the STM i.e., through the illumination of the nanogap between the plasmonically active STM tip<sup>21</sup> and the metal substrate by visible light, the plasmons can be excited and a confined, intense localized EM field can be generated at the tip apex, which can provide details to locally understand plasmon-induced changes.<sup>22-24</sup> In recent years, STM combined with optical excitation has been successfully employed for local chemical reactions assisted by LSPs.<sup>24-25</sup> With such an approach, a

certain type of chemical bond within small organic molecules such as dimethyl sulfide [S—S bond]<sup>24</sup> and oxygen (O—O bond)<sup>25-26</sup> have been activated by localized plasmons. Maintaining the typical tip-sample distance at  $\sim 1$  nm or more, the plasmonic confinement at the tip apex (that dictates the lateral distribution of the plasmonic field, typically on the order of  $\approx 5$ -10 nm)<sup>24,27</sup> remains a critical aspect in single-molecule plasmon-induced chemistry, as it can affect other molecules nearby the tip, in addition to the molecule underneath the tip. All these results lead to a very interesting query: how can we precisely control and confine the localized plasmons to activate a specific molecular site from the part of a single molecule, specifically if there

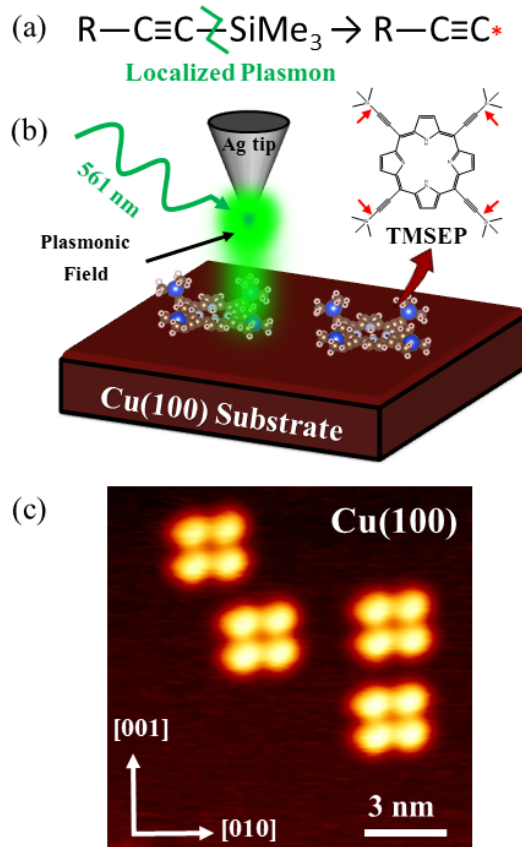


**Figure 1.** (a) Simplified scheme of the reaction. (b) Schematic illustration of the experimental setup for the real-space visualization of the plasmon-assisted site-selective activation of a single TMSEP molecule in the STM nano-junction by a Ag tip and  $Cu(100)$  surface. (inset) Chemical structure of TMSEP, (c) Constant current STM image of TMSEP.

exist multiple chemically equivalent sites within that molecule (in the order of  $\approx 1$ -2 nm)? It is particularly intriguing, as a selective chemical reaction at a specific molecular site (desired chemical bond), in the presence of multiple chemically equivalent sites inside a single molecule, lies at the heart of many nanotechnological applications, including selective heterogeneous catalysis, surface functionalization, and so forth.<sup>28-29</sup> Such controlled activation of a specific chemical bond has been achieved in some cases by tunneling electrons injected from the STM tip.<sup>30-31</sup> As an alternative option, the tip-assisted plasmon-induced reaction is also very efficient for chemical bond activation. However, due to the lateral distribution of the plasmonic field, controlling the plasmon-induced activation of a specific molecular site inside a single molecule remains extremely challenging and of tremendous fundamental importance.

We chose to investigate the carbon—silicon (C—Si) single bond activation (Figure 1a) within an individual 5,10,15,20-(tetra-trimethylsilyl)porphyrin (TMSEP, Figure 1b) molecule adsorbed on the  $Cu(100)$  surface at low temperature (78 K). The controlled activation of the C—Si bond has been a ubiquitous theme in alkyne chemistry as trimethylsilyl (TMS,  $-SiMe_3$ ) groups are employed as a masking group ( $-C\equiv C-SiMe_3$ ) for the reactive terminal alkyne ( $-C\equiv C-H$ ) in a poly-functional molecule to block its reactivity under reaction conditions. This protecting group is extremely useful to make modifications elsewhere in the molecule and can be easily activated in solution under mild conditions.<sup>32</sup> Thus, the controlled activation of such a masking group within a poly-functional single molecule holds great promise in reaction manipulation towards the desired product. The fine control of the localized plasmon to activate a selective bond can be precisely achieved by bringing the tip extremely close to the molecule for several seconds [atomistic approach, i.e., tip-sample distance ( $d$ ) is extremely small, Figure 1b], which leads to the atomic confinement of light at the tip apex.<sup>6,33</sup>

At sub-monolayer coverage of TMSEP, isolated molecules are observed (Figure 1c) as they tend to be randomly distributed across the flat  $Cu$

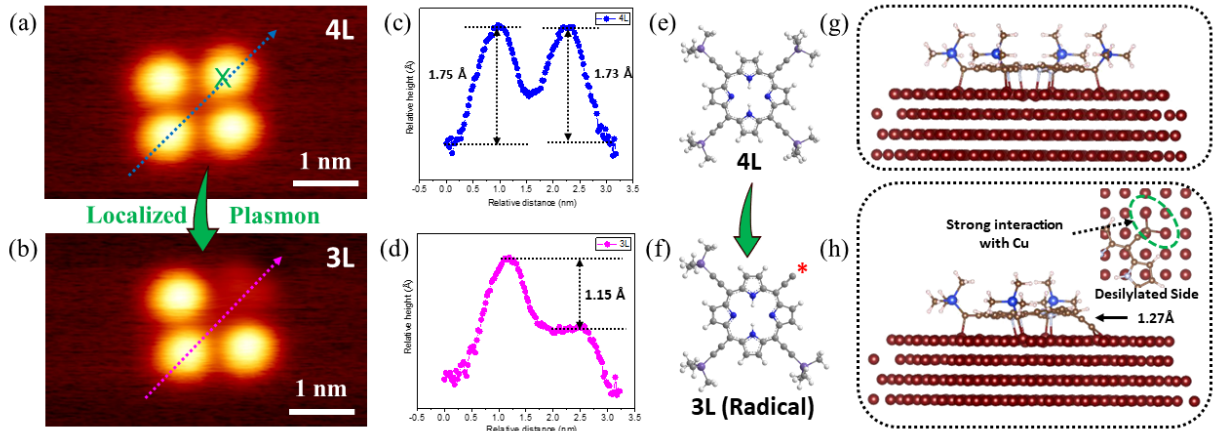


**Figure 2.** (a) and (b) STM image of 4L and 3L. (c) and (d) Relative height profile from 4L and 3L. (e) and (f) Ball-and-stick model of 4L and 3L. (g) and (h) Calculated adsorption geometry of 4L and 3L (side view).

terraces and remain separated from the neighboring molecules due to the relatively strong molecule-substrate interactions and negligible intermolecular interactions.<sup>34-36</sup> Each molecule appears as a four-lobe (4L) structure with a square shape (four bright protrusions). In order to verify whether the light can cause any chemical transformation of the TMSEP molecules during scanning, we compare an STM image of TMSEP molecules, acquired in the absence of light (Figure S2) with Figure 1c. No topographical differences are observed. From the dimensions of a single TMSEP molecule in the gas phase, we infer that the lobes correspond to the bulky TMS groups while the porphyrin backbone remains invisible, which agrees with previous studies performed on similar types of molecules.<sup>37-38</sup> We also studied the adsorbed geometry of 4L on Cu(100) using DFT calculations (Figure 2g). In agreement with the experiment, Figure 2g shows that the 4L exhibits strong interactions with the underlying Cu substrate. Specifically, the Cu atoms interact with the alkyne moieties ( $-\text{C}\equiv\text{C}-$ ), where the carbon-carbon triple bond distance is 1.27 Å compared to that of 1.22 Å in a stand-alone TMSEP molecule. The four bulky TMS groups are pointing upward, leading to the 4L structure.

In an effort to gain precise control over the localized plasmonic field that is generated at the tip apex, we positioned the Ag tip over the molecule (precisely over one lobe) and approached the tip extremely close towards the molecule for several seconds (atomistic approach. i.e.,  $d \propto \ln(V/I_t)\Phi^{1/2}\text{A}^{-1}$  where  $I_t = 5 \text{ nA}$  and  $V = 50 \text{ mV}$  in

this system).<sup>27</sup> By approaching the Ag tip extremely close over one lobe (marked by the green “x” in Figure 2a), a highly confined field is generated by LSP in the tunneling junction, resulting in the formation of a three-lobe (3L, Figure 2b) structure. As one can see in Figure 2b, the single TMSEP molecule (Figure 2a) has been transformed, showing a significantly lower apparent height of  $1.15 \pm 0.1 \text{ \AA}$  at the reacted site (Figure 2c and 2d). Following lobe dissociation, the other three lobes typically retain their original size and shape. In order to confirm the observed modification at the single-molecule level is due to LSPL, we performed controlled experiments in the dark, maintaining the same parameters ( $I_t = 5 \text{ nA}$  and  $V = 50 \text{ mV}$ ), which suggests no lobe dissociation in the absence of light (Figure S3).

Such a significant relative height difference strongly suggests that the observed topological change ( $4\text{L} \rightarrow 3\text{L}$ ) is due to the loss of one bulky TMS group. Based on that, we propose the structural model of 3L, in which one TMS moiety dissociates to generate an alkynyl radical species, while the other three TMS groups remain intact on the surface (Figure 2e and 2f). We also analyzed the adsorption configuration of 3L using DFT calculations. After the dissociation of one TMS group to create the 3L species, the adsorption geometry (3L) confirms a strong interaction of the radical with the Cu substrate while the remaining three TMS groups remain unchanged on the surface (Figure 2h). The newly generated alkynyl radical at the desilylated side can interact with the two underlying Cu atoms (inset, Figure 2h),

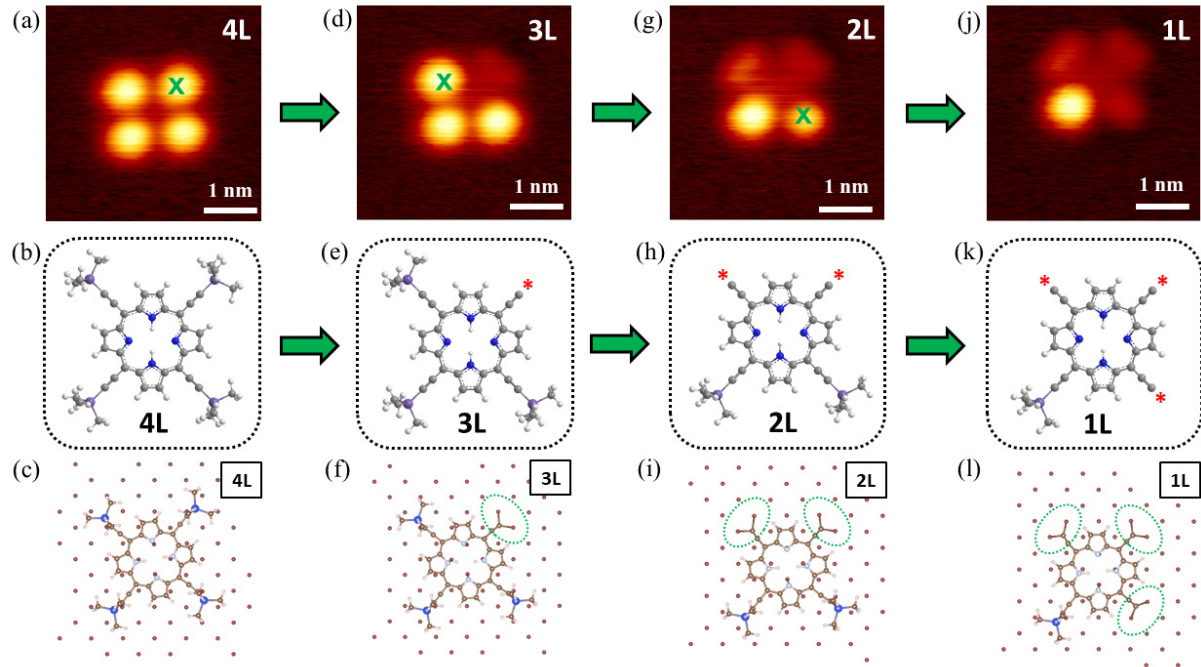


**Figure 3.** Consecutive C—Si bond dissociations from 4L→3L→2L→1L. STM image, ball-and-stick model, and calculated adsorption geometry (top view) for 4L (a, b, c), 3L (d, e, f), 2L (g, h, i), and 1L (j, k, l) respectively.

preserving the triple bond character of the adjacent alkyne group as the calculated carbon-carbon triple bond distance is 1.27 Å (more discussions in Supporting Information, Section S4). Since a single TMSEP molecule consists of other chemically indistinguishable reactive sites within a 1 nm range, the selective activation of only one site indicates that it is possible to confine the LSPs in a nano-cavity for precise plasmon-induced structure manipulation (more discussions in Supporting Information, Section S5). Furthermore, the selective activation of only one site hints towards the hot-electron transfer mechanism (analogous to the C—N bond dissociation for diazonium salts)<sup>39</sup><sup>40</sup> as the most probable mechanism for this process (more discussions in Supporting Information, Section S6). In addition to the plasmonic resonance, the chemical reaction inside the single molecule can be triggered by inelastic tunneling electrons from the STM tip, although significantly higher biases are required compared to the plasmon-induced case (see Supporting Information, Section S7)

The growing interest in chemical reaction manipulation to form different sets of products at the single-molecule level is of great importance to address many questions ranging from selective

heterogeneous catalysis to nanotechnology. In particular, if the precursor exhibits multiple chemically equivalent active sites in its structure, the desired activation of different parts of the molecule in a carefully designed sequence can lead to new unique products, which are otherwise inaccessible through conventional chemistry. Since TMSEP has four such equivalent active sites ( $-\text{C}\equiv\text{C}-\text{SiMe}_3$ ) within  $\approx 1$  nm distance, the controlled activation of multiple sites one by one to produce different types of products starting from a single TMSEP molecule offers a tremendous opportunity to manipulate a chemical reaction at the single-molecule level.

Such a scenario is illustrated in Figure 3 where the atomistic approach was followed at each step. Each irreversible change in molecular topology (consecutive molecular site activation) indicates the single molecule has undergone a certain change inside the molecule. Starting from 4L (Figure 3a and 3b), we first generate the 3L mono-radical species (Figure 3d and 3e). The corresponding calculated adsorption geometry (top view) of 4L and 3L is presented in Figures 3c and 3f, respectively. Next, in order to activate another molecular site adjacent to the desilylated side, we apply one more atomistic treatment on 3L (marked

by the green “x” in Figure 3d). The topological feature changed to a two-lobe structure (2L, Figure 3g), suggesting the dissociation of another adjacent C—Si bond to produce a bi-radical species (proposed model, Figure 3h). As seen in the simulated adsorption configuration for 2L (Figure 3i), both the alkynyl radicals now interact with two underlying Cu atoms each while the other two unreacted TMS groups remain unchanged. In addition to the formation of the 2L structure by activating two adjacent molecular sites, two opposite sites can also be activated by positioning the STM tip at the desired site and following the atomistic approach, as shown in Figure S8. With one more atomistic approach (denoted by the green “x” in Figure 3g), we can now construct a one-lobe structure (1L, Figure 3j), by activating three molecular sites. Figure 3k illustrates the proposed model for 1L, dissociating three C—Si bonds from a single molecule to generate a tri-alkynyl radical species. The calculated adsorption geometry (Figure 3l) again confirms an identical interaction of the radical sides with the Cu surface, as now all three alkynyl radicals are connected with two underlying Cu atoms each, leaving one TMS group intact. Furthermore, our simulation suggests that the triple-bond character in all three alkyne moieties (adjacent to the radical sites) remains preserved. Thus, the sequential plasmonic action only precisely affects the C—Si bonds without disturbing the electronic nature of adjacent carbon–carbon triple bonds. Additional STM images showing 2L and 0L species are presented in Figure S9. Together these observations indicate that each plasmonic treatment of single molecules provides identical molecular fragments (alkynyl radicals in this case), even if, the molecular active sites are  $\approx$   $< 1$  nm away from each other. Therefore, out of four chemically indistinguishable parts inside a single molecule, the selective activation of one or multiple molecular sites implies the attainment of plasmonic nano-confinement in manipulating the desired chemical reaction.

In conclusion, the selective chemical bond activation inside a single molecule induced by a nano-confined plasmon is reported. In terms of manipulating a certain plasmon-assisted chemical reaction, this unprecedented level of precision is achieved through an atomistic approach, thereby confining light to a nano-cavity at the tip apex. Furthermore, multiple chemically equivalent

reaction sites are sequentially activated within a single TMSEP molecule in a controlled fashion, suggesting a potential and broad application towards plasmon-induced molecular engineering of poly-functional molecular structure.

## ASSOCIATED CONTENT

### Supporting Information

Experimental Section; Real-space observation of plasmon-induced chemical change; Atomistic approach in the absence of light; Additional details for 3L; Plasmonic distribution with varying tip-sample distance; Plausible mechanism of C—Si bond dissociation on Cu(100), Bias-induced C—Si bond dissociation; STM image of 2L with two opposite C—Si bonds get dissociated; Additional STM images of 2L and 0L.

## AUTHOR INFORMATION

### Corresponding Authors

**Linfei Li** - Department of Chemistry, University of Illinois Chicago, Chicago, Illinois 60607, United States.

\*E-mail: [linfei@uic.edu](mailto:linfei@uic.edu)

**Nan Jiang** - Department of Chemistry, University of Illinois Chicago, Chicago, Illinois 60607, United States.

\*E-mail: [njiang@uic.edu](mailto:njiang@uic.edu)

### Authors

**Sayantan Mahapatra** - Department of Chemistry, University of Illinois Chicago, Chicago, Illinois 60607, United States.

**Jeremy F. Schultz** - Department of Chemistry, University of Illinois Chicago, Chicago, Illinois 60607, United States.

**Xu Zhang** - Department of Physics and Astronomy, California State University, Northridge, California 91330, United States.

## ORCID

Sayantan Mahapatra: 0000-0002-7332-196X

Jeremy F. Schultz: 0000-0003-2231-6797

Linfei Li: 0000-0002-5217-3005

Xu Zhang: 0000-0002-6491-3234

Nan Jiang: 0000-0002-4570-180X

## Notes

The authors declare no competing financial interest.

## ACKNOWLEDGMENTS

N.J. acknowledge support from National Science Foundation (CHE-1944796). X.Z. acknowledges support from National Science Foundation (DMR-1828019).

## REFERENCES:

- (1) Aslam, U.; Rao, V. G.; Chavez, S.; Linic, S., Catalytic Conversion of Solar to Chemical Energy on Plasmonic Metal Nanostructures. *Nat. Catal.* **2018**, *1*, 656-665.
- (2) Ding, S.-Y.; Yi, J.; Li, J.-F.; Ren, B.; Wu, D.-Y.; Panneerselvam, R.; Tian, Z.-Q., Nanostructure-Based Plasmon-Enhanced Raman Spectroscopy for Surface Analysis of Materials. *Nat. Rev. Mater.* **2016**, *1*, 16021.
- (3) Jain, P. K.; Huang, X.; El-Sayed, I. H.; El-Sayed, M. A., Noble Metals on the Nanoscale: Optical and Photothermal Properties and Some Applications in Imaging, Sensing, Biology, and Medicine. *Acc. Chem. Res.* **2008**, *41*, 1578-1586.
- (4) Lal, S.; Link, S.; Halas, N. J., Nano-Optics from Sensing to Waveguiding. *Nat. Photonics* **2007**, *1*, 641-648.
- (5) Langer, J., et al., Present and Future of Surface-Enhanced Raman Scattering. *ACS Nano* **2020**, *14*, 28-117.
- (6) Mahapatra, S.; Li, L.; Schultz, J. F.; Jiang, N., Tip-Enhanced Raman Spectroscopy: Chemical Analysis with Nanoscale to Angstrom Scale Resolution. *J. Chem. Phys.* **2020**, *153*, 010902.
- (7) Mayer, K. M.; Hafner, J. H., Localized Surface Plasmon Resonance Sensors. *Chem. Rev.* **2011**, *111*, 3828-3857.
- (8) Brongersma, M. L.; Halas, N. J.; Nordlander, P., Plasmon-Induced Hot Carrier Science and Technology. *Nat. Nanotech.* **2015**, *10*, 25-34.
- (9) Zhang, Y.; He, S.; Guo, W.; Hu, Y.; Huang, J.; Mulcahy, J. R.; Wei, W. D., Surface-Plasmon-Driven Hot Electron Photochemistry. *Chem. Rev.* **2018**, *118*, 2927-2954.
- (10) Kazuma, E.; Kim, Y., Mechanistic Studies of Plasmon Chemistry on Metal Catalysts. *Angew. Chem. Int. Ed.* **2019**, *58*, 4800-4808.
- (11) Li, L.; Mahapatra, S.; Liu, D.; Lu, Z.; Jiang, N., On-Surface Synthesis and Molecular Engineering of Carbon-Based Nanoarchitectures. *ACS Nano* **2021**, *15*, 3578-3585.
- (12) Mukherjee, S.; Zhou, L.; Goodman, A. M.; Large, N.; Ayala-Orozco, C.; Zhang, Y.; Nordlander, P.; Halas, N. J., Hot-Electron-Induced Dissociation of H<sub>2</sub> on Gold Nanoparticles Supported on SiO<sub>2</sub>. *J. Am. Chem. Soc.* **2014**, *136*, 64-67.
- (13) Zhou, L., et al., Quantifying Hot Carrier and Thermal Contributions in Plasmonic Photocatalysis. *Science* **2018**, *362*, 69.
- (14) Mukherjee, S.; Libisch, F.; Large, N.; Neumann, O.; Brown, L. V.; Cheng, J.; Lassiter, J. B.; Carter, E. A.; Nordlander, P.; Halas, N. J., Hot Electrons Do the Impossible: Plasmon-Induced Dissociation of H<sub>2</sub> on Au. *Nano Lett.* **2013**, *13*, 240-247.
- (15) Kazuma, E.; Kim, Y., Scanning Probe Microscopy for Real-Space Observations of Local Chemical Reactions Induced by a Localized Surface Plasmon. *Phys. Chem. Chem. Phys.* **2019**, *21*, 19720-19731.
- (16) Kazuma, E.; Jung, J.; Ueba, H.; Trenary, M.; Kim, Y., Stm Studies of Photochemistry and Plasmon Chemistry on Metal Surfaces. *Prog. Surf. Sci.* **2018**, *93*, 163-176.
- (17) Doppagne, B.; Chong Michael, C.; Bulou, H.; Boeglin, A.; Scheurer, F.; Schull, G., Electrofluorochromism at the Single-Molecule Level. *Science* **2018**, *361*, 251-255.

(18) Doppagne, B.; Neuman, T.; Soria-Martinez, R.; López, L. E. P.; Bulou, H.; Romeo, M.; Berciaud, S.; Scheurer, F.; Aizpurua, J.; Schull, G., Single-Molecule Tautomerization Tracking through Space- and Time-Resolved Fluorescence Spectroscopy. *Nature Nanotech.* **2020**, *15*, 207-211.

(19) Hung, T.-C.; Kiraly, B.; Strik, J. H.; Khajetoorians, A. A.; Wegner, D., Plasmon-Driven Motion of an Individual Molecule. *Nano Lett.* **2021**, *21*, 5006-5012.

(20) Neuman, T.; Esteban, R.; Casanova, D.; García-Vidal, F. J.; Aizpurua, J., Coupling of Molecular Emitters and Plasmonic Cavities Beyond the Point-Dipole Approximation. *Nano Lett.* **2018**, *18*, 2358-2364.

(21) Mahapatra, S.; Li, L.; Schultz, J. F.; Jiang, N., Methods to Fabricate and Recycle Plasmonic Probes for Ultrahigh Vacuum Scanning Tunneling Microscopy-Based Tip-Enhanced Raman Spectroscopy. *J. Raman Spectrosc.* **2021**, *52*, 573-580.

(22) Chauchaiyakul, S.; Setiadi, A.; Krukowski, P.; Catalan, F. C. I.; Akai-Kasaya, M.; Saito, A.; Hayazawa, N.; Kim, Y.; Osuga, H.; Kuwahara, Y., Nanoscale Dehydrogenation Observed by Tip-Enhanced Raman Spectroscopy. *J. Phys. Chem. C* **2017**, *121*, 18162-18168.

(23) Szczerbiński, J.; Gyr, L.; Kaelin, J.; Zenobi, R., Plasmon-Driven Photocatalysis Leads to Products Known from E-Beam and X-Ray-Induced Surface Chemistry. *Nano Lett.* **2018**, *18*, 6740-6749.

(24) Kazuma, E.; Jung, J.; Ueba, H.; Trenary, M.; Kim, Y., Real-Space and Real-Time Observation of a Plasmon-Induced Chemical Reaction of a Single Molecule. *Science* **2018**, *360*, 521.

(25) Kazuma, E.; Lee, M.; Jung, J.; Trenary, M.; Kim, Y., Single-Molecule Study of a Plasmon-Induced Reaction for a Strongly Chemisorbed Molecule. *Angew. Chem. Int. Ed.* **2020**, *59*, 7960-7966.

(26) Lin, C.; Ikeda, K.; Shiota, Y.; Yoshizawa, K.; Kumagai, T., Real-Space Observation of Far- and near-Field-Induced Photolysis of Molecular Oxygen on an Ag(110) Surface by Visible Light. *J. Chem. Phys.* **2019**, *151*, 144705.

(27) Böckmann, H.; Gawinkowski, S.; Waluk, J.; Raschke, M. B.; Wolf, M.; Kumagai, T., Near-Field Enhanced Photochemistry of Single Molecules in a Scanning Tunneling Microscope Junction. *Nano Lett.* **2018**, *18*, 152-157.

(28) Killelea, D. R.; Campbell, V. L.; Shuman, N. S.; Utz, A. L., Bond-Selective Control of a Heterogeneously Catalyzed Reaction. *Science* **2008**, *319*, 790.

(29) Li, S.; Czap, G.; Wang, H.; Wang, L.; Chen, S.; Yu, A.; Wu, R.; Ho, W., Bond-Selected Photodissociation of Single Molecules Adsorbed on Metal Surfaces. *Phys. Rev. Lett.* **2019**, *122*, 077401.

(30) Anggara, K.; Huang, K.; Leung, L.; Chatterjee, A.; Cheng, F.; Polanyi, J. C., Bond Selectivity in Electron-Induced Reaction Due to Directed Recoil on an Anisotropic Substrate. *Nature Commun.* **2016**, *7*, 13690.

(31) Schuler, B.; Fatayer, S.; Mohn, F.; Moll, N.; Pavliček, N.; Meyer, G.; Peña, D.; Gross, L., Reversible Bergman Cyclization by Atomic Manipulation. *Nature Chem.* **2016**, *8*, 220-224.

(32) Larson, G. L., Some Aspects of the Chemistry of Alkynylsilanes. *Synthesis (Stuttg)* **2018**, *50*, 2433-2462.

(33) Lee, J.; Crampton, K. T.; Tallarida, N.; Apkarian, V. A., Visualizing Vibrational Normal Modes of a Single Molecule with Atomically Confined Light. *Nature* **2019**, *568*, 78-82.

(34) Mahapatra, S.; Schultz, J. F.; Ning, Y.; Zhang, J.-L.; Jiang, N., Probing Surface Mediated Configurations of Nonplanar Regioisomeric Adsorbates Using Ultrahigh Vacuum Tip-Enhanced Raman Spectroscopy. *Nanoscale* **2019**, *11*, 19877-19883.

(35) Rojas, G., et al., Self-Assembly and Properties of Nonmetalated Tetraphenyl-Porphyrin on Metal Substrates. *J. Phys. Chem. C* **2010**, *114*, 9408-9415.

(36) Jiang, N.; Zhang, Y. Y.; Liu, Q.; Cheng, Z. H.; Deng, Z. T.; Du, S. X.; Gao, H. J.; Beck, M. J.; Pantelides, S. T., Diffusivity Control in Molecule-on-Metal Systems Using Electric Fields. *Nano Lett.* **2010**, *10*, 1184-1188.

(37) Kawai, S.; Krejčí, O.; Foster, A. S.; Pawlak, R.; Xu, F.; Peng, L.; Orita, A.; Meyer, E., Diacetylene Linked Anthracene Oligomers Synthesized by One-Shot Homocoupling of Trimethylsilyl on Cu(111). *ACS Nano* **2018**, *12*, 8791-8797.

(38) Gao, H.-Y., et al., Intermolecular on-Surface  $\sigma$ -Bond Metathesis. *J. Am. Chem. Soc.* **2017**, *139*, 7012-7019.

(39) Bléreau, P.; Bastide, M.; Gam-Derouich, S.; Martin, P.; Bonnet, R.; Lacroix, J.-C., Plasmon-Induced Grafting in the Gap of Gold Nanoparticle Dimers for Plasmonic Molecular Junctions. *ACS Appl. Nano Mater.* **2020**, 3, 7789-7794.

(40) Nguyen, V.-Q.; Ai, Y.; Martin, P.; Lacroix, J.-C., Plasmon-Induced Nanolocalized Reduction of Diazonium Salts. *ACS Omega* **2017**, 2, 1947-1955.

TOC Graphic:

